

# Thermodynamic Calculation of Phase Diagram in the Bi–In–Sb Ternary System

Yuwen Cui<sup>1</sup>, Satoru Ishihara<sup>2</sup>, Xing Jun Liu<sup>1</sup>, Ikuo Ohnuma<sup>1</sup>, Ryosuke Kainuma<sup>1</sup>, Hiroshi Ohtani<sup>3</sup> and Kiyohito Ishida<sup>1</sup>

<sup>1</sup>Department of Materials Science, Graduate School of Engineering, Tohoku University, Sendai 980-8579, Japan

<sup>2</sup>Japan Science and Technology Corporation

<sup>3</sup>Center for Interdisciplinary Research, Tohoku University, Sendai 980-8578, Japan

A thermodynamic description of the Bi–In–Sb ternary system of lead-free solder alloys using the CALPHAD (Calculation of Phase Diagram) method is presented. Phase equilibria information such as vertical sections, liquidus projection and thermochemical quantities were calculated and compared with the experimental data. The calculated and experimental data are in excellent agreement in most cases.

(Received March 11, 2002; Accepted May 2, 2002)

**Keywords:** thermodynamic calculation, lead-free solder, calculation of phase diagram, bismuth, indium, antimony

## 1. Introduction

During the past decade, increasing efforts have been made to search for suitable Pb-free solders as substitutes for the conventional Pb–Sn eutectic alloys because of environmental and health concerns regarding lead usage.<sup>1)</sup> Many investigations have indicated that the needed Pb-free solders are likely to be multi-component alloys because the melting temperatures of binary candidates are either too high or low, with respect to the conventional Sn–Pb solders. Therefore, alloy design is important for the development of Pb-free soldering alloys in multi-component system.

The CALPHAD (Calculation of Phase Diagram) is an effective method for alloy design and has widely been used in development of new materials.<sup>2)</sup> In the frame of the CALPHAD technique, the present authors have developed a thermodynamic database for micro-solders with eight elements Ag, Bi, Cu, In, Pb, Sb, Sn and Zn,<sup>3,4)</sup> which can provide the information of not only phase equilibria but also physical properties of liquid phase such as surface tension and viscosity. Since Bi, In and Sb are important elements for the development of Pb-free solders, the thermodynamic description of the Bi–In–Sb system is required for the accurate prediction of melting temperature, phase constitution, solidification behavior *etc.* in the multi-component alloy systems. In addition, some investigations<sup>5,6)</sup> have revealed that the InSb<sub>1-x</sub>Bi<sub>x</sub> compound ( $x = 0.01-0.02$ ) is suitable for utilization in the middle infra-red detection field, while the InSb gap was reduced and the photosensitivity spectral maximum was shifted toward the long-wave region by doping InSb with Bi into the Sb site to form solid solutions of InSb<sub>1-x</sub>Bi<sub>x</sub>. An appropriate thermodynamic description of the Bi–In–Sb system is thus of fundamental importance from a technical perspective.

## 2. Evaluation of Previous Works

### 2.1 Binary subsystems

An analytic calculation for the Bi–In system was previously reported by Chevalier.<sup>7)</sup> Shortly afterward, he offered

a revised version in Scientific Group Thermodata Europe (SGTE) databank.<sup>8)</sup> Unfortunately, in the calculation running with these parameters, the (In) solid solution was found to be stable at the Bi-rich portion of the temperature range extending from 125 to 100°C, which is thermodynamic improbable. In addition, a large discrepancy between the predicted eutectoid temperature (42°C) and the experimental value (49°C) was found, namely, as large as, 7°C. Therefore, further modification is needed.

A detailed review of experimental data and descriptions of thermodynamic model have already been given in the assessment by Chevalier.<sup>7)</sup> It is thus unnecessary to repeat them here. The modified parameters by this work are listed in Table 1. Comparison between the present calculation and that from Chevalier<sup>7)</sup> is shown in Fig. 1. As can be seen, a great improvement on the two above-mentioned problems was achieved.

The parameters of the In–Sb binary system are available from the SGTE database, which were developed by scientific collaboration.<sup>9)</sup>

Many investigators<sup>10-15)</sup> have performed the thermodynamic calculation on the system Bi–Sb. The critical assessment by Feutelais *et al.*<sup>14)</sup> was selected from the SGTE database. However, a better fit with the solidus was given by a recent work of Ohtani and Ishida<sup>15)</sup> who additionally employed their own new experimental data. This updated set of parameters was taken into account in the present work.

### 2.2 Ternary system

Several experimental studies have focused on the Bi–In–Sb ternary system. In an early research of the Bi–In–Sb ternary system by Peretti,<sup>16)</sup> the InSb–InBi cross section exhibited a true quasi-binary studied by thermal analysis, X-ray diffraction and microscopic examinations. Employing the same methods, Peretti<sup>17,18)</sup> carried out two consecutive works in which a number of isopleths were well determined. InSb was found to appear as a dominant primary phase upon cooling from the liquid state in most cases. From these results, he established two partial idealized three-dimensional space models of both InSb–InBi–Bi–Sb and InSb–InBi–In sub-systems

Table 1 Summary of the parameters assessed in present work and the binary parameters from the selected literature. (Values for solution phases are given in J/mol of atoms, and in J/mol formula units for the intermediate phases.)

System	Phase	Parameters	Reference
Bi-In	Liquid	$L(\text{Liquid, Bi, In; } 0) = -7165.05 - 0.3605^*T$ $L(\text{Liquid, Bi, In; } 1) = 1503.8 - 0.59659^*T$ $L(\text{Liquid, Bi, In; } 2) = 1221.15 - 0.7515^*T$ $L(\text{Liquid, Bi, In; } 3) = -1627 + 1.34243^*T$	This work This work This work This work
	Rhombohedral_A7	$G(\text{Rhombohedral\_A7, In; } 0) = 4184 + \text{GHSERIN}$ $L(\text{Rhombohedral\_A7, Bi, In; } 0) = 0$ $L(\text{Rhombohedral\_A7, Bi, In; } 1) = 22500$	This work 8) 8)
	Tetragonal_A6	$G(\text{tetragonal\_A6, Bi; } 0) = 5575.382 + \text{GHSERBI}$ $L(\text{tetragonal\_A6, Bi, In; } 0) = 2294.79 - 17.10^*T$ $L(\text{tetragonal\_A6, Bi, In; } 1) = 1644.36$	This work This work This work
	BiIn	$L(\text{BiIn, Bi, In; } 0) = -732.2 - 3.7873^*T + .5^*\text{GHSERBI} + .5^*\text{GHSERIN}$	8)
	BiIn <sub>2</sub>	$G(\text{BiIn}_2, \text{Bi, In; } 0) = -477 - 4.17277^*T + .33333^*\text{GHSERBI} + .66667^*\text{GHSERIN}$	This work
	Bi <sub>3</sub> In <sub>5</sub>	$G(\text{Bi}_3\text{In}_5, \text{Bi, In; } 0) = -543.9 - 4.09864^*T + .375\text{GHSERBI} + .625^*\text{GHSERIN}$	8)
	$\epsilon$	$G(\epsilon, \text{Bi; } 0) = 5575.38 + \text{GHSERBI}$ $G(\epsilon, \text{In; } 0) = +\text{GHSERIN}$ $L(\epsilon, \text{Bi, In; } 0) = -757.76 - 19.47^*T$ $L(\epsilon, \text{Bi, In; } 1) = -2970.16$	This work 7) This work This work
Bi-Sb	Liquid	$L(\text{Liquid, Bi, Sb; } 0) = 2230 + .061^*T$	15)
	Rhombohedral_A7	$L(\text{Rhombohedral\_A7, Bi, Sb; } 0) = 10150 - 6.3^*T$ $L(\text{Rhombohedral\_A7, Bi, Sb; } 1) = 150$	15)
In-Sb	Liquid	$L(\text{Liquid, In, Sb; } 0) = -25631.2 + 102.9324^*T - 13.45816^*T^*\text{LN}(T)$ $L(\text{Liquid, In, Sb; } 1) = -2115.41 + 1.31907^*T$ $L(\text{Liquid, In, Sb; } 2) = 2908.9835$	9)
	InSb	$L(\text{InSb, In, Sb; } 0) = -15849.3 + .293139^*T + 1.293581^*T^*\text{LN}(T)$	9)
Bi-In-Sb	Liquid	$L(\text{Liquid, Bi, In, Sb; } 0) = 11850.55 + 2.094^*T$ $L(\text{Liquid, Bi, In, Sb; } 1) = 12526.62 - 54.038^*T$ $L(\text{Liquid, Bi, In, Sb; } 2) = -6951.95 + 55.83^*T$	This work This work This work

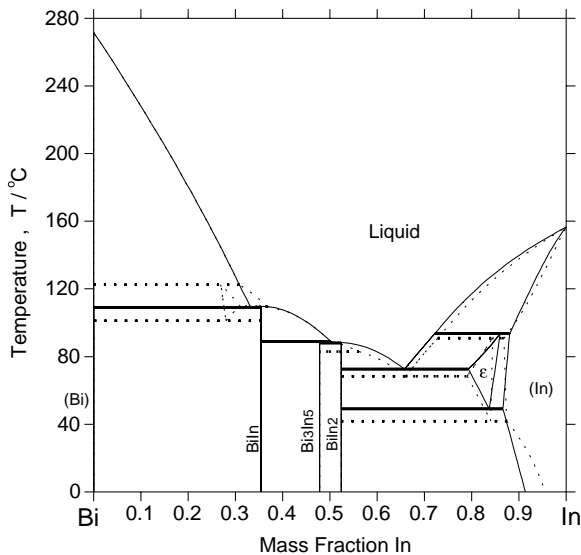


Fig. 1 Calculated Bi-In phase diagrams: present work (solid line), Chevalier<sup>7)</sup> (dashed line).

and an entire liquid projection. As these works<sup>16-18)</sup> provided a comprehensive depiction of the Bi-In-Sb phase relation, the data reported were thus adopted in the present work.

On the basis of electron diffraction phase analysis, Palatnik *et al.*<sup>19)</sup> investigated the stability of metastable phases in the In-Bi-Sb system and constructed a topological diagram for ternary alloys related to room temperature. This topological diagram, however, encountered some deviations from the phase rule since what they have studied was not an equilibrium but a quasi-equilibrium phase diagram. Their data were therefore excluded in this work.

Using the DTA measurements on the single crystals samples, Joukoff and Jean-Louis<sup>5)</sup> obtained an indication that the InBi solubility limit in InSb is about 2 at%. With the aid of the DTA and local X-ray spectral analysis (LXSA), Ufimtsevm *et al.*<sup>6)</sup> revealed that the InSb-In<sub>2</sub>Bi cross section was a quasi-binary characterized by a simple eutectic type. The latter research group also measured the solubility of Bi in the compound InSb over the cross sections of InSb-Bi, InSb-InBi and InSb-In<sub>2</sub>Bi. The data reported on the InSb-In<sub>2</sub>Bi cross section were adopted in this work, but the solubility of Bi in the InSb compound from the above two sources were only used in the initial calculation.

Contributions from three groups<sup>20-22)</sup> to the study of the thermodynamic properties of the Bi-In-Sb system were found in the literature. With a high temperature calorimeter, Predel and Gerdes<sup>20)</sup> determined the enthalpy changes on mixing molten InSb with liquid Bi at 612°C. The enthalpy of

mixing derived shows a positive deviation from ideality with a maximum at about 560 J/mol. The thermodynamic properties of the InSb–Bi liquid were distinctly calculated on the assumption of the formation of associate InSb and the liquidus curve in the pseudobinary system InSb–Bi was derived. By an electromotive forces method, Goryacheva *et al.*<sup>21)</sup> obtained the partial thermodynamic properties of In in liquid and heterogeneous In–Bi–Sb mixtures, and used them for calculating integral properties of alloys. They also fitted these data by a simplex lattice method to yield the liquidus surface and composition dependence of enthalpy and Gibbs excess energy in the whole concentration region. Recently, Kameda *et al.*<sup>22)</sup> carried out the emf measurement on fifteen alloys using a zirconia electrolyte by determining the activity of In in liquid at 613–906°C. Correlating the binary data and the least square fitting method, they consequently derived the isoactiv-

ity curves at 727 and 827°C. It is noted that the measured mixing enthalpy of liquid by Predel and Gerdes<sup>20)</sup> and the activity of In in liquid by Kameda *et al.*<sup>22)</sup> are essentially consistent, and thus these two sets of data were preferred for this work. Only the original experimental data from Goryacheva *et al.*,<sup>21)</sup> *i.e.* partial mixing enthalpy of In in liquid were considered in this work, in which the data at the constant Bi/Sb ratios 1:1 and 1:2 possessing comparative large uncertainties with those at the 2:1 ratio, as indicated by Goryacheva *et al.*, were given a low weight.

### 3. Thermodynamic Model and Optimization Procedure

The substitutional solution model was used to describe the tetragonal-In, rhombohedral-(Bi, Sb),  $\epsilon$  and liquid phases. The model yields the following expression for the Gibbs

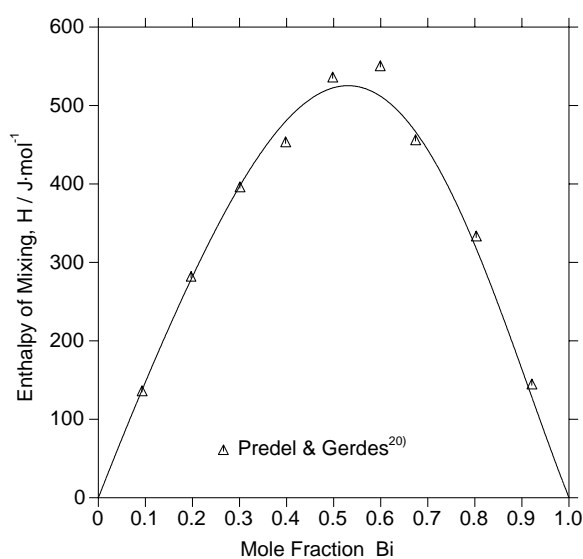


Fig. 2 Calculated enthalpy of mixing in molten InSb with liquid at 612°C, in comparison with the experimental data.

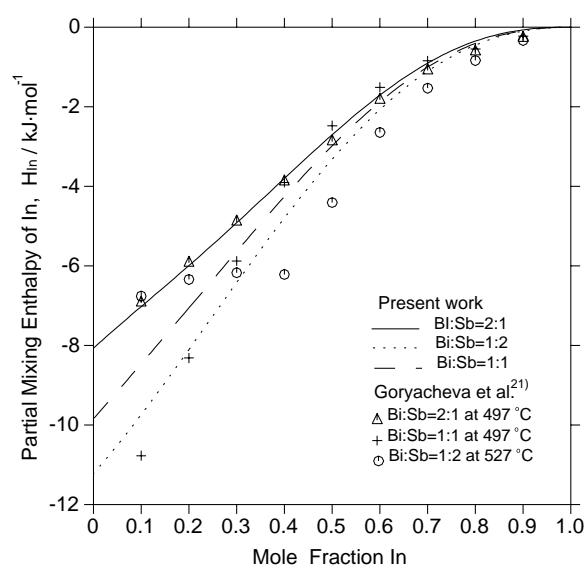


Fig. 4 Calculated partial molar mixing enthalpy of In in the liquid phase compared with the experimental data.

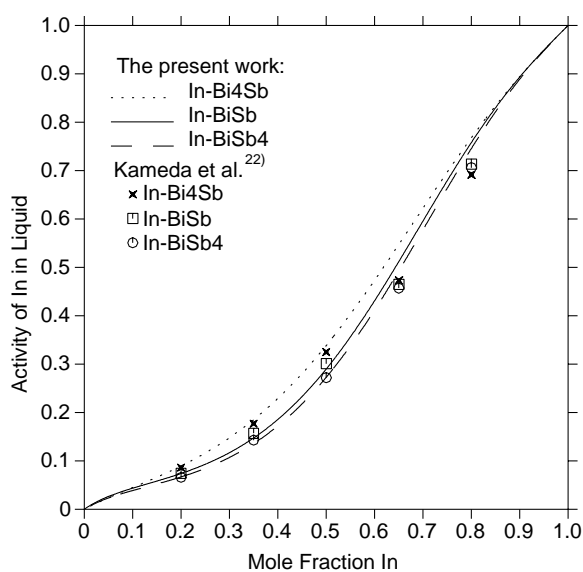


Fig. 3 Calculated activity of In in liquid Bi–In–Sb alloys at 727°C, in comparison with the experimental data.

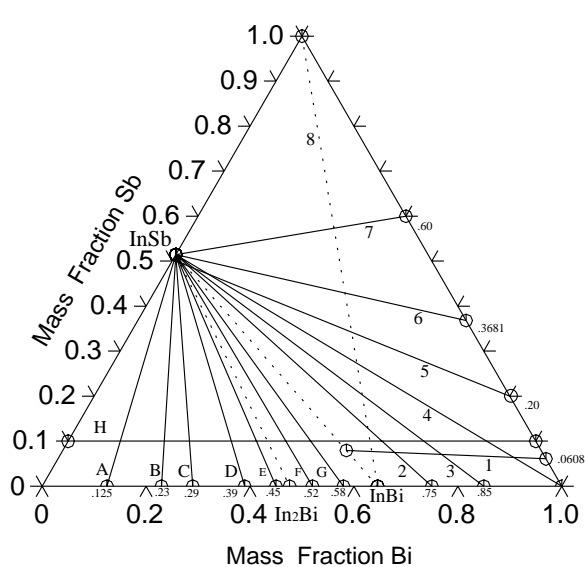


Fig. 5 Locations of the calculated vertical sections of the Bi–In–Sb system in this work.

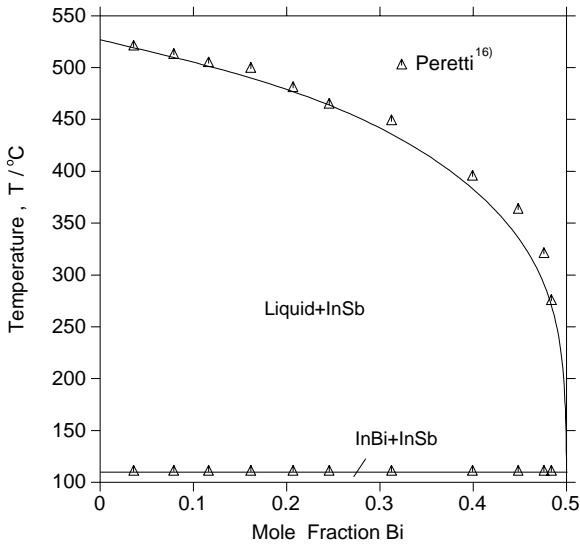


Fig. 6 Calculated InSb–InBi vertical section compared with the experimental data.

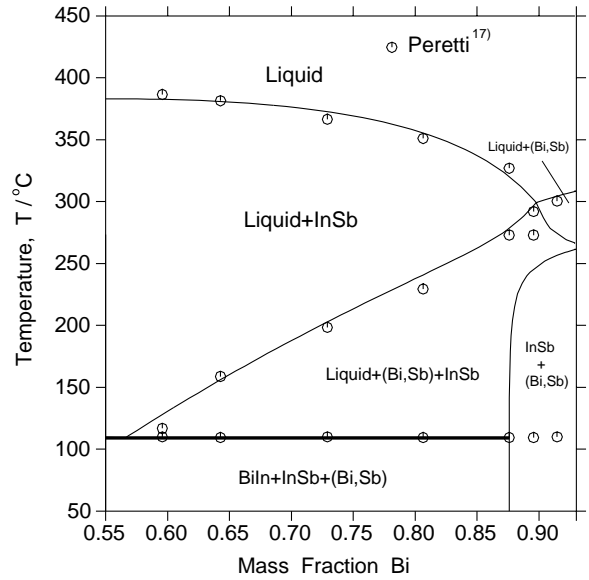


Fig. 8 Calculated vertical section #1 compared with the experimental data. (See Figure 5 for location).

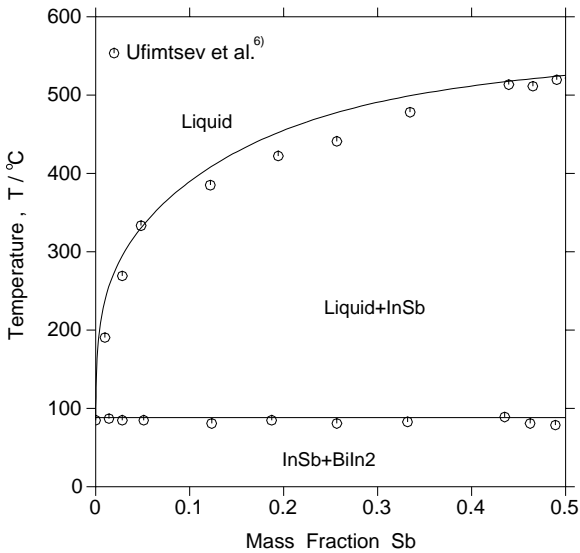


Fig. 7 Calculated InSb–BiIn<sub>2</sub> vertical section compared with the experimental data.

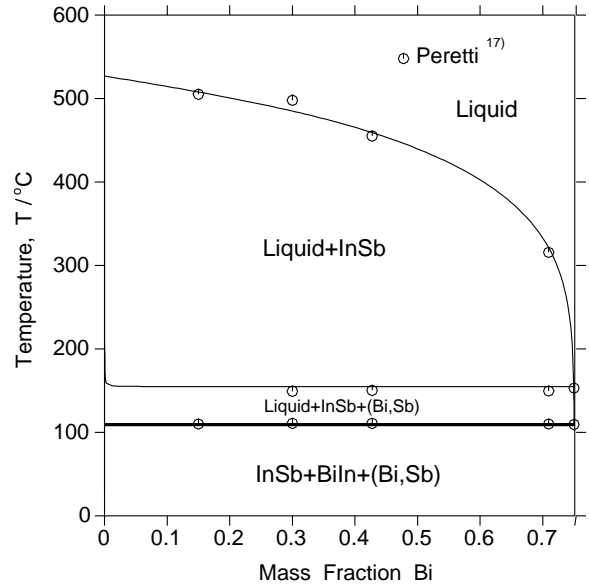


Fig. 9 Calculated vertical section #2 compared with the experimental data. (See Fig. 5 for location).

energy:

$$G_m = x_{Bi} G_{Bi} + x_{In} G_{In} + x_{Sb} G_{Sb} + RT(x_{Bi} \ln x_{Bi} + x_{In} \ln x_{In} + x_{Sb} \ln x_{Sb}) + {}^{ex}G_m \quad (1)$$

The parameter  $G_i$  is the Gibbs energy of pure component  $i$  which can be taken from the database.<sup>23)</sup> The excess energy  ${}^{ex}G_m$  can be derived from the binary excess Gibbs energy  ${}^{ex}G_{i,j}$  ( $i, j = Bi, In$  and  $Sb$ ) using Muggianu's extrapolation model:<sup>24)</sup>

$${}^{ex}G_m = \sum_{i=1}^2 \sum_{j=i+1}^3 [x_i x_j / (V_{i,j} V_{j,i})] {}^{ex}G_{i,j} + x_{Bi} x_{In} x_{Sb} (x_{Bi} L_{Bi} + x_{In} L_{In} + x_{Sb} L_{Sb}) \quad (2)$$

$L_i$  denotes the ternary interaction parameter, and the terms  $V_{i,j}$  and  $V_{j,i}$  are represented by

$$V_{i,j} = \frac{1 + x_i - x_j}{2} \quad \text{and} \quad V_{j,i} = \frac{1 + x_j - x_i}{2} \quad (3)$$

Among the remaining intermediate phases, namely BiIn, BiIn<sub>2</sub>, Bi<sub>3</sub>In<sub>5</sub> and InSb, only the InSb phase was confirmed to have a solubility range in the ternary system, although a negligible one. During the optimization, however, it was found that even a very small solubility of Bi in InSb would significantly deteriorate the overall accuracy of the prediction and thus such solubility data were finally discarded. Fortunately, such a simplification has a minor effect on the phase equilibria of the system.

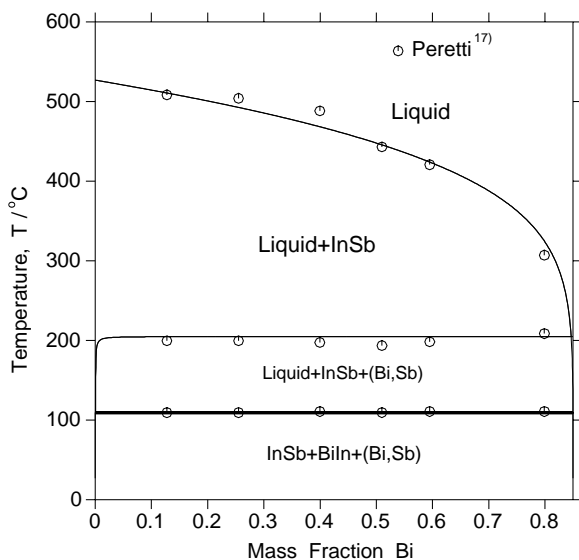


Fig. 10 Calculated vertical section #3 compared with the experimental data. (See Fig. 5 for location).

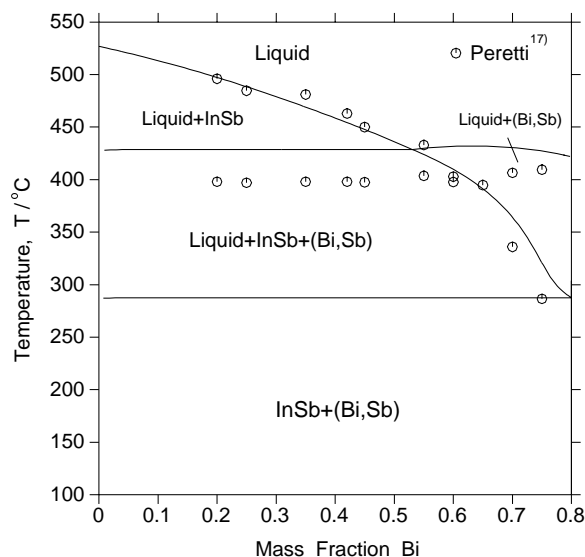


Fig. 12 Calculated vertical section #5 compared with the experimental data. (See Fig. 5 for location).

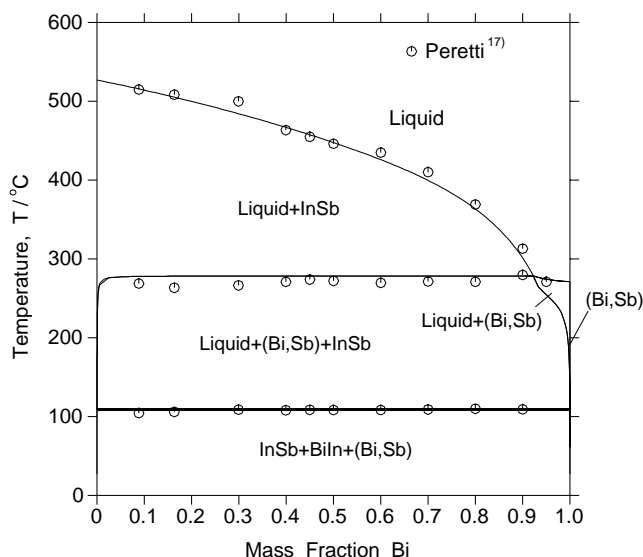


Fig. 11 Calculated vertical section #4 (InSb–Bi) compared with the experimental data. (See Fig. 5 for location).

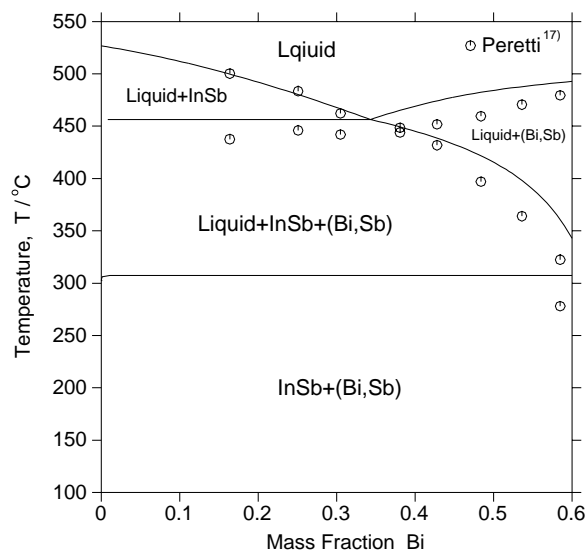


Fig. 13 Calculated vertical section #6 compared with the experimental data. (See Fig. 5 for location).

The optimization of parameters was carried out using the Parrot module in Thermo-Calc program developed by Sundman *et al.*<sup>25)</sup>

#### 4. Results and Discussion

The assessed parameters in this work, as well as the binary parameters used in present work<sup>9,15)</sup> are summarized in Table 1. The tabulation indicates that only the ternary interaction energies for liquid, besides the binary parameters, were sufficient for reliable calculation.

Figures 2 and 3 illustrate the calculated mixing enthalpy between InSb with liquid bismuth at 612°C and the activity of In in liquid, respectively. The calculations correspond very well with those measured experimentally.<sup>20,22)</sup> But an unacceptable convergence of the optimization was encountered

when the data from Goryacheva *et al.*<sup>21)</sup> were simultaneously taken into account. This problem was readily solved as soon as their data at the Bi/Sb ratios 1:1 and 1:2 (appearing as unusual curvatures) were given a low weight and the temperature terms were introduced to the interaction energies of the liquid. Such treatments were further found to enhance the fitness to liquidus. Comparison between the calculated partial molar mixing enthalpy of In in liquid and the experimental data<sup>21)</sup> is presented in Fig. 4. Apparently, the computed data at the 2:1 ratio compare nicely with the experimental points, but there are some discrepancies remaining in those at the 1:1 and 1:2 ratios which were given the low weight.

To facilitate the following discussion, Fig. 5 graphically shows the locations of the cross sections which are theoretically compared and confirmed in this work, namely, #1 through #8, and #A through #G. in Figs. 6 through 15, the

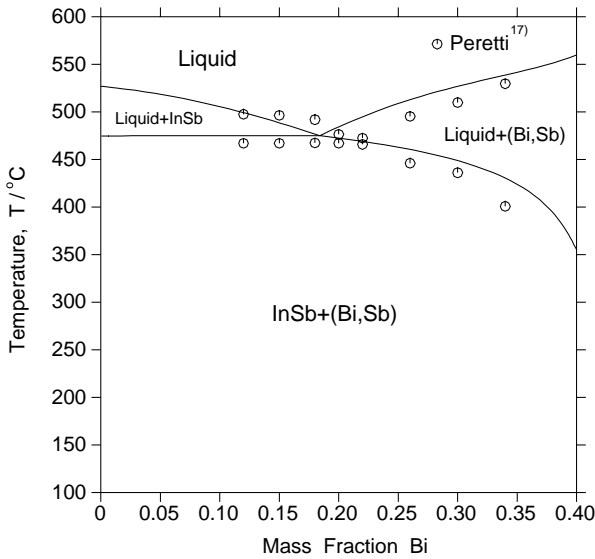


Fig. 14 Calculated vertical section #7 compared with the experimental data. (See Fig. 5 for location).

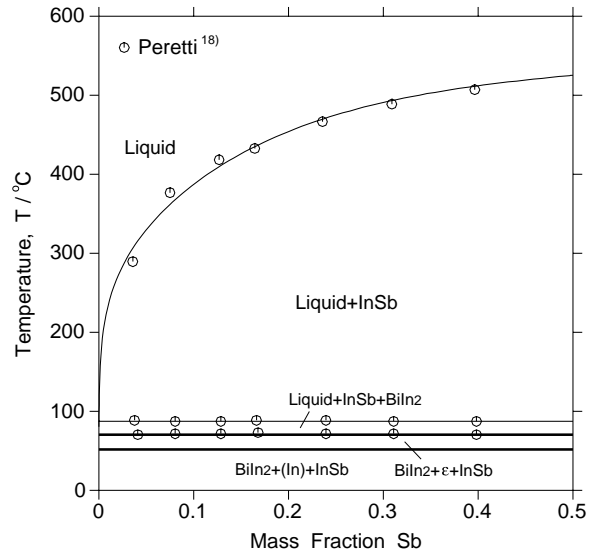


Fig. 16 Calculated vertical section #E compared with the experimental data. (See Fig. 5 for location).

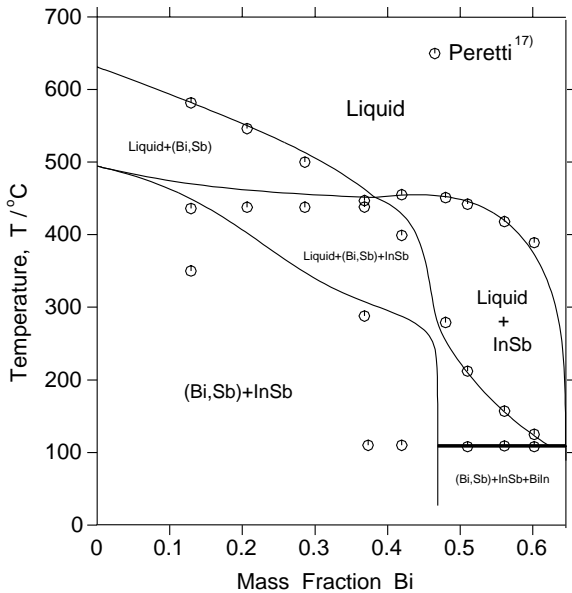


Fig. 15 Calculated vertical section #8 compared with the experimental data. (See Fig. 5 for location).

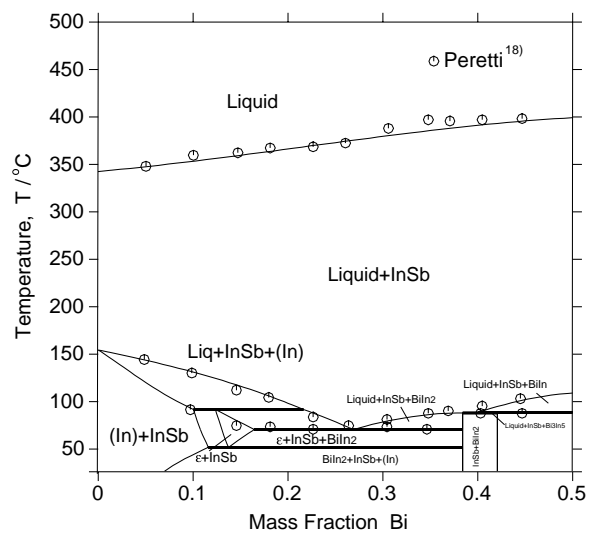


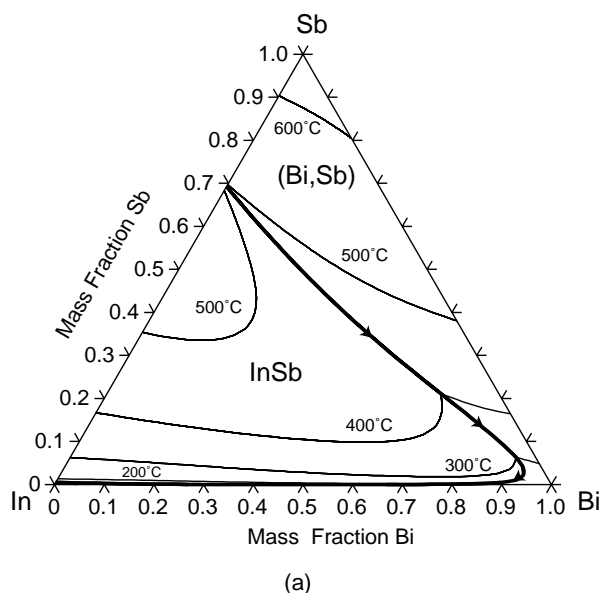
Fig. 17 Calculated vertical section #H (with 10 mass% Sb) in comparison with the experimental data.

calculated cross sections #1 through #8 are compared with the experimental values.<sup>6,16,17</sup> The agreements in Sections #1 to #4 are excellent. Major differences which occur for the liquidus and solidus pertain to the rhombohedral-(Bi, Sb) phase in Sections #5 to #8, as seen from Figs. 12 through 15. However, a previous study on the Bi–Sn binary system<sup>26</sup> suggested the diffusion rate in the rhombohedral-(Bi, Sb) solid solution is not very high, and most investigators<sup>17</sup> have found it necessary to perform heat treatment for long periods to equilibrate its alloys. It is thus reasonable to assume that obvious undercooling may be involved in the cooling DTA measurements of the related alloys by Peretti.<sup>17</sup> It is sufficient to note that the calculated results happen to be located somewhat above the experimental values in those phase regions. As a consequence, no extra attempt to give a better

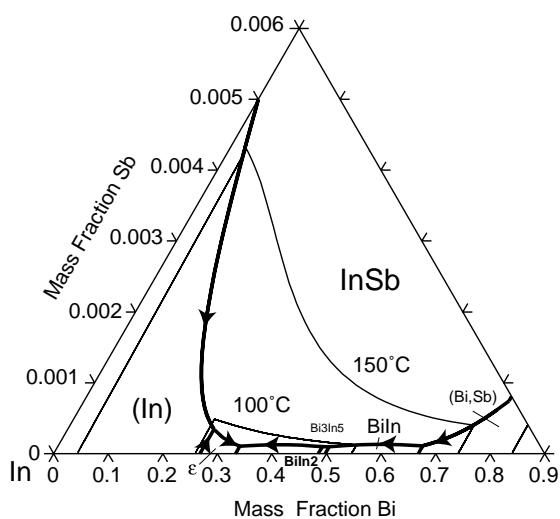
fitness was finally made in this work, apart from the incorporation of a rhombohedral-(In, Sb) parameter which can bring limited improvement.

Calculation of these sections #A through #G exhibited a very similar appearance, *i.e.* an uninterrupted liquidus running from the freezing temperature of InSb to a point located very close to the respective Bi–In binary alloys. The calculations represent the experimental data very well in all cases of sections #A through #G. To reserve space, only the calculated cross section #E, along with the superimposed the measured points,<sup>18</sup> is given in this paper as an example (see Fig. 16).

Figure 17 presents excellent agreement between the calculated cross section at 10 mass% Sb and the experimental values.<sup>18</sup> Two ternary peritectic reactions,  $L + Bi_3In_5 \rightleftharpoons InSb + BiIn_2$  and  $L + BiIn \rightleftharpoons InSb + Bi_3In_5$ , were shown to take place at two very close temperatures, 88.1 and 88.8°C, which were not distinguished by Peretti. The advantage of



(a)

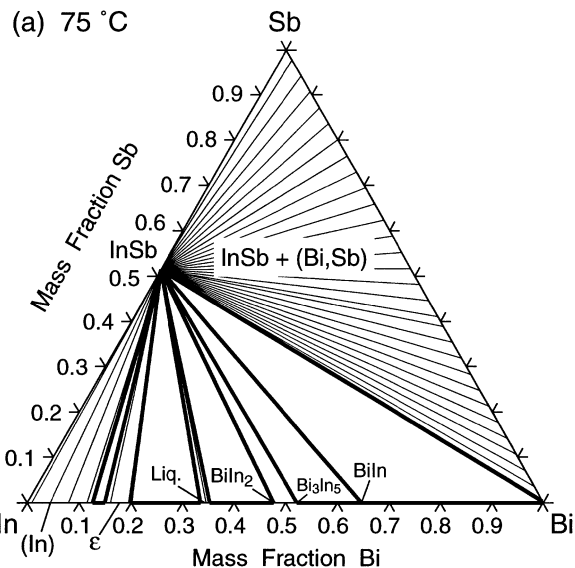


(b)

Fig. 18 (a) Calculated liquidus projection of the Bi–In–Sb ternary system; (b) an enlarged portion near the Bi–In binary axis.

the phase diagram calculation thus becomes manifest in this instance.

Figure 18(a) depicts an entire calculated liquidus projection of the Bi–In–Sb system accompanying by iso-liquidus at the 100°C temperature interval, Fig. 18(b) showing better enhancement of the area adjacent to the Bi–In binary edge. It can be seen that, totally, six ternary invariant reactions exist in the Bi–In–Sb ternary system, but with exception, occur about only negligible Sb contents. Clearly, this picture provides insight into the phase relation of the Bi–In binary edge that is sorely lacking in the literature and which is necessary to understand the stable phase equilibrium under extreme conditions. In more depth, the results imply that Bi only slightly suppresses the ternary melting temperature on the In-rich side, whereas the liquidus temperature increases significantly with an increase of Sb concentration. Table 2 summarizes the calculated ternary invariant reactions, as well as the available experimental information. Very good agree-



(b) 120 °C

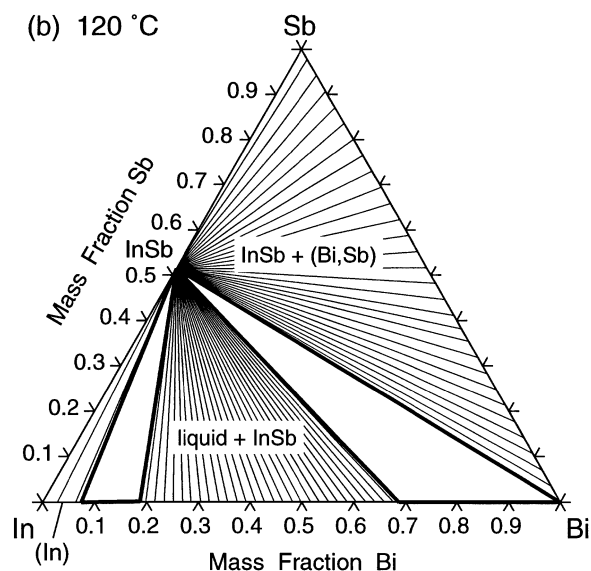


Fig. 19 The predicted Bi–In–Sb isothermal sections at (a) 75°C and (b) 120°C.

ment is observed for all the comparable reactions.

Figure 19 shows the calculated isothermal diagrams at 75 and 120°C to highlight the isothermal feature of the system.

## 5. Conclusion

A thermodynamic description of the Bi–In–Sb ternary system was developed using the CALPHAD method in this work. A number of the thermochemical quantities and cross sections were calculated and compared with the experimental data. They are in excellent agreement in most cases. The present calculation can serve as a guideline for practical application and for a border ternary system in the extrapolation to high order systems.

## Acknowledgments

This work was supported by Grants-in-Aid for Scientific Research from the Ministry of Education, Science, Sports and

Table 2 Comparison of the calculated invariant reactions with the literature data.

Reaction	Type	$T$ (°C)	Composition of the liquid phase (mass%)			Reference
			Bi	In	Sb	
$L \Leftrightarrow \varepsilon + \text{InSb} + \text{BiIn}_2$	Eutectic	71.8*				18) (Exp.)
		70.6	33.3227	66.6668	0.0011	This work (Cal.)
$L + (\text{In}) \Leftrightarrow \varepsilon + \text{InSb}$	Peritectic	91.3*				18) (Exp.)
		91.7	26.8069	73.1586	0.0034	This work (Cal.)
$L + \text{Bi}_3\text{In}_5 \Leftrightarrow \text{InSb} + \text{BiIn}_2$	Peritectic	87.9*				18) (Exp.)
		88.1	48.5029	51.4871	0.0010	This work (Cal.)
$L + \text{BiIn} \Leftrightarrow \text{InSb} + \text{Bi}_3\text{In}_5$	Peritectic	89				18) (Exp.)
		88.8	49.7652	50.2251	0.0010	This work (Cal.)
$L + (\text{Bi}, \text{Sb}) \Leftrightarrow \text{BiIn} + \text{InSb}$	Eutectic	109				18) (Exp.)
	Peritectic	109.2	33.1853	66.8038	0.0011	This work (Cal.)

\*Average values among the DTA data given in Ref. 18).

Culture, Japan.

## REFERENCES

- 1) M. Abtew and G. Selvaduray: *Mater. Sci. Eng. R* **27** (2000) 95–141.
- 2) N. Saunders and A. P. Miodownik: *CALPHAD* (Lausanne, Switzerland Pergamon, 1998).
- 3) I. Ohnuma, X. J. Liu, H. Ohtani and K. Ishida: *J. Electron. Mater.* **28** (1999) 1164–1171.
- 4) X. J. Liu, S. L. Chen, I. Ohnuma, K. Ishida and Y. A. Chang: *Mechanics and Material Engineering for Science and Experiments*, ed. by Y. C. Zhou, Y. Gu and Z. Li (Science Press, 2001) pp. 334–337.
- 5) B. Joukoff and A. M. Jean-Louis: *J. Crystal Growth* **12** (1972) 169–172.
- 6) V. B. Ufimtsevm, V. G. Zinov'ev and M. R. Raukman: *Inorg. Mater.* **15** (1979) 1371–1374.
- 7) P.-Y. Chevalier: *CALPHAD* **12** (1988) 383–392.
- 8) B. Sundman: SGTE binary databank, (1992).
- 9) I. Ansara, C. Chatillon, H. L. Lukas, T. Nishizawa, H. Ohtani, K. Ishida, M. Hillert, B. Sundman, B. B. Argent, A. Watson, T. G. Chart and T. Anderson: *CALPHAD* **18** (1994) 177–222.
- 10) F. Ajersch and I. Ansara: Rapport L.T.P.C.M. TM01, E.N.S.E.E.G., St. Martin d'Herès, (1974).
- 11) A. B. Bhatia and N. H. Pelton: *Can. Metall. Quart.* **14** (1975) 213–219.
- 12) S. S. Balakrishna and A. K. Mallik: *Sci. Forum* **3** (1985) 405–417.
- 13) A. D. Pelton and C. W. Bale: *Metall. Trans.* **17A** (1986) 1057–1063.
- 14) Y. Feutelais, G. Morgant, J. R. Didry and J. Schnitter: *CALPHAD* **16** (1992) 111–116.
- 15) H. Ohtani and K. Ishida: *J. Electron. Mater.* **23** (1994) 747–755.
- 16) E. A. Peretti: *Trans. Metall. AIME* **212** (1958) 79.
- 17) E. A. Peretti: *Trans. Am. Soc. Met.* **52** (1960) 1046–1058.
- 18) E. A. Peretti: *Trans. Am. Soc. Met.* **54** (1961) 12–19.
- 19) L. S. Palatnik, V. M. Kosevich and L. V. Tyrina: *Phys. Met. Metallography* **11** (1961) 75–80.
- 20) B. Predel and F. Gerdes: *J. Less-Comm. Met.* **59** (1978) 153–164.
- 21) V. I. Goryacheva, S. F. Pashin and V. A. Geiderikh: *Vestn. Mosk. Univ. Ser. 2, Khim* **26** (1986) 142–150.
- 22) K. Kameda and T. Kon: *J. Jpn. Inst. Metals* **61** (1997) 444–448.
- 23) A. Dinsdale: *CALPHAD* **15** (1991) 317–425.
- 24) Y. M. Muggianu, M. Gambino and J. P. Bros: *J. Chim. Phys.* **72** (1975) 83–88.
- 25) B. Sundman, B. Jansson and J. O. Andersson: *CALPHAD* **9** (1985) 153–190.
- 26) J. L. Haughton and A. Prince: *The Constitutional Diagram of Alloys: A Bibliography*, (Institute of Metals, 1956) p. 82.